Nuclear Structure of ^{154,156}Dy Isotopes

Salah A. Eid[1], Sohair M. Diab[2]

[1]Faculty of Engineering, Phys. Dept., Ain Shams University, Cairo, Egypt.
[2]Faculty of Education, Phys. Dept., Ain Shams University, Cairo, Egypt.
E-mail: mppe2@yahoo.co.uk

The Interacting Boson Approximation model, *IBA*-1, has been used in studying the nuclear structure of ^{154,156}Dy. The excited positive and negative parity states, potential energy surfaces, $V(\beta,\gamma)$, electromagnetic transition probabilities, $B(E1)$, $B(E2)$, back bending, staggering effect, $\Delta I = 1$, and electric monopole strength, $X(E0/E2)$, were calculated successfully. The calculated values are compared to the available experimental data and show reasonable agreement. The energy and electromagnetic transition probabilities ratios as well as the contour plot of the potential energy surfaces show that the ^{156}Dy nucleus is an $X(5)$ candidate.

1 Introduction

The nuclear shape and shape phase transitions in the rare earth dysprosium isotopes have been investigated by many authors theoretically and experimentally. Theoretically, analytical solution of the Bohr Hamiltonian derived with the Titz-Hua potential [1] as well as Bohr-Mottelson Hamiltonian [2,3] were used in calculating energy levels, spin, parity and electromagnetic ratios. The effect of the nuclear structure on the α-decay are investigated by many authors [4-6] and found that the shape and deformation has an effect on the branching ratio as well as the change in the half-life of α-emission. Experimentally, the low-lying positive and negative parity states were produced in the ^{148}Nd (^{12}C,4n), ^{155}Gd (^{3}He,4n), E= 37.5 MeV, ^{122}Sn (^{36}S,4n), E= 165 MeV and ^{114}Cd (^{48}Ca,6n), E= 215 MeV [7-9] reactions. The levels' energy, spin, parity, γ-bands, branching ratios, level energy differences between the positive and negative parity bands, octupole deformation, γ-γ coincidences and angular distribution were measured. Conversion electrons were detected by mini-orange spectrometer, $E0$ transitions were observed and the strength of the electric monopole transitions were calculated [10].

$X(5)$ is the critical point symmetry of phase transition between $U(5)$ and $SU(3)$ nuclei. The aim of the present work is to:

1. Calculate the potential energy surfaces, $V(\beta,\gamma)$;
2. Calculate the levels' energy and electromagnetic transition rates $B(E1)$ and $B(E2)$;
3. Show $X(5)$ symmetry to ^{156}Dy;
4. Calculate the back bending;
5. Calculate the staggering effect, and
6. Calculate the electric monopole strength, $X(E0/E2)$.

2 Interacting Boson Approximation model *IBA*-1

2.1 Levels' energy

The *IBA*-1 Hamiltonian [11] employed on ^{154,156}Dy, in the present calculation, is:

$$\begin{aligned} H &= EPS \cdot n_d + PAIR \cdot (P \cdot P) \\ &+ \frac{1}{2}\, ELL \cdot (L \cdot L) + \frac{1}{2}\, QQ \cdot (Q \cdot Q) \\ &+ 5\, OCT \cdot (T_3 \cdot T_3) + 5\, HEX \cdot (T_4 \cdot T_4)\,, \end{aligned} \tag{1}$$

where

$$P \cdot P = \frac{1}{2}\begin{bmatrix} \left\{(s^\dagger s^\dagger)_0^{(0)} - \sqrt{5}(d^\dagger d^\dagger)_0^{(0)}\right\} x \\ \left\{(ss)_0^{(0)} - \sqrt{5}(\tilde{d}\tilde{d})_0^{(0)}\right\} \end{bmatrix}_0^{(0)}, \tag{2}$$

$$L \cdot L = -10\sqrt{3}\left[(d^\dagger \tilde{d})^{(1)} x\, (d^\dagger \tilde{d})^{(1)}\right]_0^{(0)}, \tag{3}$$

$$Q \cdot Q = \sqrt{5}\begin{bmatrix} \left\{(S^\dagger \tilde{d} + d^\dagger s)^{(2)} - \frac{\sqrt{7}}{2}(d^\dagger \tilde{d})^{(2)}\right\} x \\ \left\{(s^\dagger \tilde{d} + +\tilde{d}s)^{(2)} - \frac{\sqrt{7}}{2}(d^\dagger \tilde{d})^{(2)}\right\} \end{bmatrix}_0^{(0)}, \tag{4}$$

$$T_3 \cdot T_3 = -\sqrt{7}\left[(d^\dagger \tilde{d})^{(2)} x\, (d^\dagger \tilde{d})^{(2)}\right]_0^{(0)}, \tag{5}$$

$$T_4 \cdot T_4 = 3\left[(d^\dagger \tilde{d})^{(4)} x\, (d^\dagger \tilde{d})^{(4)}\right]_0^{(0)}. \tag{6}$$

and n_d is the number of d bosons; $P \cdot P$, $L \cdot L$, $Q \cdot Q$, $T_3 \cdot T_3$ and $T_4 \cdot T_4$ represent pairing, angular momentum, quadrupole, octupole and hexadecupole interactions respectively between the bosons; EPS is the boson energy; and $PAIR$, ELL, QQ, OCT, HEX are the strengths of the pairing, angular momentum, quadrupole, octupole and hexadecupole interactions respectively, Table 1.

nucleus	*EPS*	*PAIR*	*ELL*	*QQ*	*OCT*	*HEX*	*E2SD*(*eb*)	*E2DD*(*eb*)
^{154}Dy	0.6240	0.000	0.0084	−0.0244	0.0000	0.0000	0.1510	−0.4467
^{156}Dy	0.4450	0.000	0.0084	−0.0244	0.0000	0.0000	0.1274	−0.3769

Table 1: Parameters used in *IBA*-1 Hamiltonian (all in MeV).

nucleus	$E_{4_1^+}/E_{2_1^+}$	$E_{6_1^+}/E_{2_1^+}$	$E_{8_1^+}/E_{2_1^+}$	$E_{0_2^+}/E_{2_1^+}$	$E_{6_1^+}/E_{0_2^+}$	$E_{0_3^+}/E_{2_1^+}$	$BE2(4_1^+ - 2_1^+)/BE2(2_1^+ - 0_1^+)$
^{154}Dy	2.09	3.12	4.86	2.12	1.46	2.95	1.91
^{156}Dy	2.86	5.36	8.43	6.15	0.87	8.78	1.56
$X(5)$	3.02	5.83	9.29	5.65	1.53	6.03	1.58

Table 2: Energy and transition probability ratios.

2.2 Transition rates

The electric quadrupole transition operator employed is:

$$T^{(E2)} = E2SD \cdot (s^{\dagger}\tilde{d} + d^{\dagger}s)^{(2)} + \\ + \frac{1}{\sqrt{5}}\, E2DD \cdot (d^{\dagger}\tilde{d})^{(2)} . \tag{7}$$

E2SD and *E2DD* are adjustable parameters.

The reduced electric quadrupole transition rates between $I_i \to I_f$ states are given by:

$$B\,(E_2, I_i - I_f) = \frac{[< I_f \parallel T^{(E_2)} \parallel I_i >]^2}{2I_i + 1} . \tag{8}$$

3 Results and discussion

3.1 The potential energy surfaces

The potential energy surfaces [12], $V(\beta, \gamma)$, as a function of the deformation parameters β and γ are calculated using:

$$E_{N_\Pi N_\nu}(\beta,\gamma) = <N_\pi N_\nu;\beta\gamma\,|H_{\pi\nu}|N_\pi N_\nu;\beta\gamma> = \\ = \zeta_d(N_\nu N_\pi)\beta^2(1+\beta^2) + \beta^2(1+\beta^2)^{-2}\times \\ \times\left\{kN_\nu N_\pi[4 - (\bar{X}_\pi\bar{X}_\nu)\beta\cos 3\gamma]\right\} + \\ + \left\{[\bar{X}_\pi\bar{X}_\nu\beta^2] + N_\nu(N_\nu - 1)\left(\frac{1}{10}\,c_0 + \frac{1}{7}\,c_2\right)\beta^2\right\} , \tag{9}$$

where

$$\bar{X}_\rho = \left(\frac{2}{7}\right)^{0.5} X_\rho , \qquad \rho = \pi \text{ (proton) or } \upsilon \text{ (neutron)} , \tag{10}$$

and ζ_d : the energy of d bosons.

The calculated potential energy surfaces, $V(\beta, \gamma)$, are presented in Figs. 1, 2. Fig. 1 shows that ^{154}Dy is a vibrational-like nucleus, U(5), while ^{156}Dy nucleus is deviated from vibrational-like to rotational-like with slight prolate deformation, SU(3), Fig. 2. The levels' energy, transition probability ratios presented in Table 2, as well as the potential energy surfaces, are in favour to consider ^{156}Dy as an $X(5)$ candidate.

$I_i^+\ I_f^+$	B (E2)	$I_i^-\ I_f^+$	B (E1)
$2_1\ 0_1$	0.4744	$1_1\ 0_1$	0.0282
$2_2\ 0_1$	0.0100	$1_1\ 0_2$	0.1336
$2_2\ 0_2$	0.3040	$3_1\ 2_1$	0.1683
$3_1\ 2_1$	0.0198	$3_1\ 2_2$	0.0658
$4_1\ 2_1$	0.9074	$3_2\ 2_1$	0.0069
$3_1\ 2_2$	0.2666	$3_2\ 2_2$	0.0235
$4_2\ 4_1$	0.1409	$3_2\ 2_3$	0.1520
$4_2\ 2_1$	0.0017	$5_1\ 4_1$	0.3035
$4_2\ 2_2$	0.5520	$5_1\ 4_2$	0.0698
$6_1\ 4_1$	1.1581	$7_1\ 6_1$	0.4380
$6_2\ 4_1$	0.0005	$7_1\ 6_2$	0.0665
$6_2\ 4_2$	0.8200	$9_1\ 8_1$	0.5734
$8_1\ 6_1$	1.2916	$9_1\ 8_2$	0.0610
$8_1\ 6_2$	0.0700	$9_2\ 8_1$	0.1750
$8_1\ 6_3$	0.0641	$9_2\ 8_2$	0.3501
$8_2\ 6_2$	0.9584	$9_2\ 8_3$	0.2144
$10_1\ 8_1$	1.3384	$11_1\ 10_1$	0.7103
$10_1\ 8_2$	0.0579	$11_1\ 10_2$	0.0543

Table 3: Calculated $B(E2)$ and $B(E1)$ in ^{154}Dy.

3.2 Energy spectra and electric transition rates

The energy of the positive and negative parity states of isotopes ^{154,156}Dy are calculated using computer code PHINT [11]. A comparison between the experimental spectra [13,14] and our calculations, using values of the model parameters given in Table 1 for the ground state, $\beta 1$, $\beta 2$, $\gamma 1$ and $\gamma 2$ bands are illustrated in Figs. 3, 4. The agreement between the calculated levels' energy and their corresponding experimental values are fair, but they are slightly higher especially for the higher excited states. We believe this is due to the change of the projection of the angular momentum which is due mainly to band crossing. Fig. 5 shows the position of $X(5)$ and $E(5)$ between the other types of nuclei.

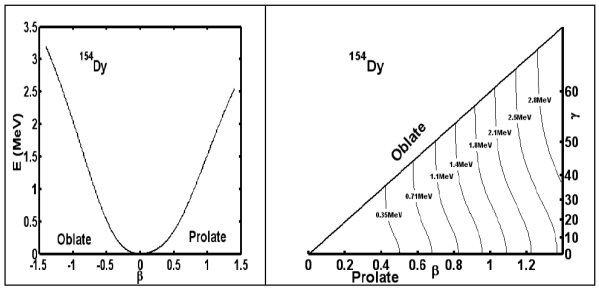

Fig. 1: Potential energy surfaces for ^{154}Dy.

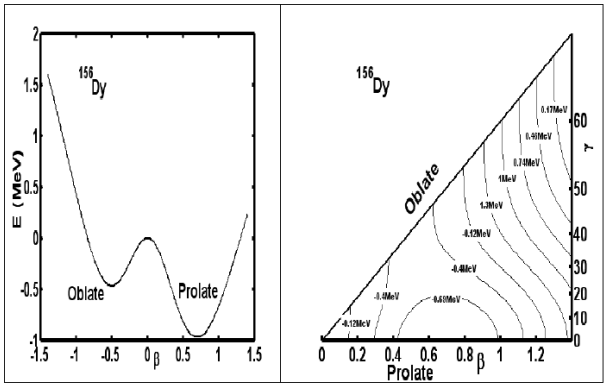

Fig. 2: Potential energy surfaces for ^{156}Dy.

I_i^+ I_f^+	B (E2)	I_i^- I_f^+	B (E1)
2_1 0_1	0.7444	1_1 0_1	0.1309
2_2 0_1	0.0023	1_1 0_2	0.0696
2_2 0_2	0.4652	3_1 2_1	0.2353
3_1 2_1	0.0169	3_1 2_2	0.0854
4_1 2_1	1.1073	3_2 2_1	0.0481
3_1 2_2	0.0026	3_2 2_2	0.0092
4_2 4_1	0.0356	3_2 2_3	0.0110
4_2 2_1	0.0016	5_1 4_1	0.3934
4_2 2_2	0.0041	5_1 4_2	0.0778
6_1 4_1	1.2446	7_1 6_1	0.5149
6_2 4_1	0.0007	7_1 6_2	0.0675
6_2 4_2	0.9083	9_1 8_1	0.6377
8_1 6_1	1.3003	9_1 8_2	0.0585
8_1 6_2	0.0410	9_2 8_1	0.0129
8_1 6_3	0.0162	9_2 8_2	0.3474
8_2 6_2	0.9817	9_2 8_3	0.2687
10_1 8_1	1.3025	11_1 10_1	0.7631
10_1 8_2	0.0332	11_1 10_2	0.0507

Table 4: Calculated $B(E1)$ and $B(E2)$ in ^{156}Dy.

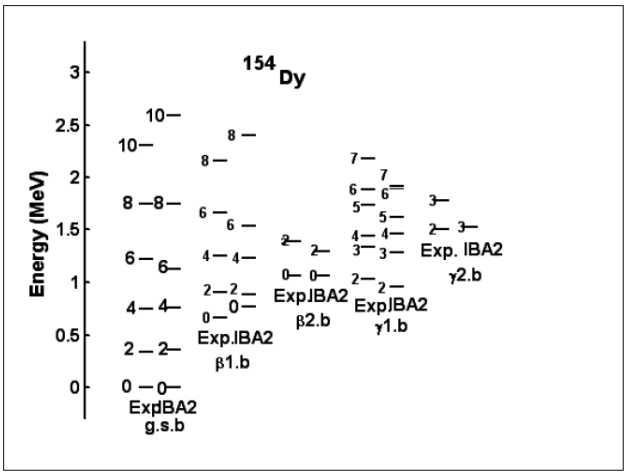

Fig. 3: Experimental[13] and calculated levels' energy.

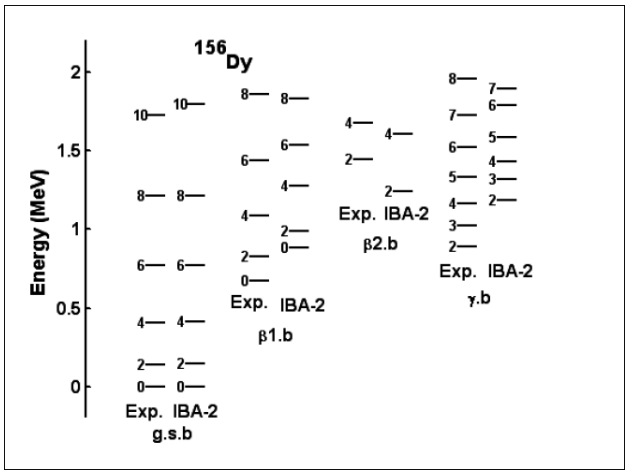

Fig. 4: Experimental[14] and calculated levels' energy.

Unfortunately there is no available measurements of electromagnetic transition rates $B(E2)$ for ^{154,156}Dy nuclei. The only measured values of $B(E2, 2_1^+ \to 0_1^+)$ for ^{154,156}Dy [15] are used in normalizing our calculated values presented in Tables 3, 4. Also, there is no experimental data available for $B(E1, I^- \to I^+)$ for normalization. Parameters *E2SD* and *E2DD* displayed in Table 1 are used in the computer code FBEM [11] for calculating the electromagnetic transition rates. No new parameters are introduced for calculating electromagnetic transition rates $B(E1)$ and $B(E2)$ of intraband and interband.

3.3 Staggering effect

The presence of positive and negative parity states has encouraged us to study the staggering effect [16] for ^{154,156}Dy isotopes using staggering functions (11) and (12) with the

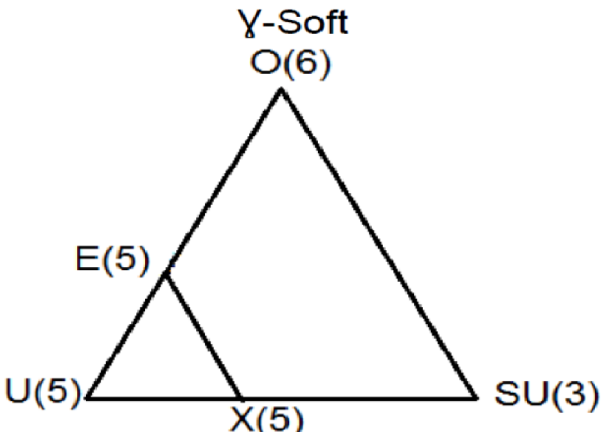

Fig. 5: Triangle showing the position of $X(5)$ and $E(5)$.

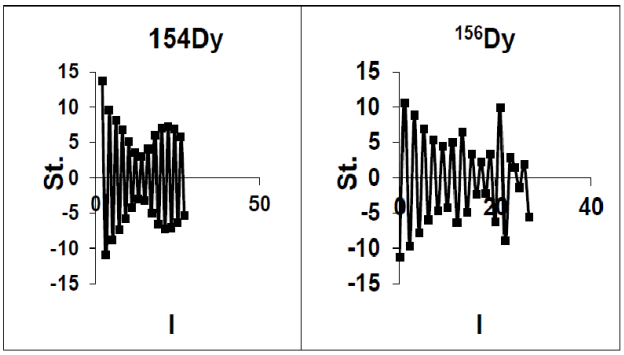

Fig. 6: Staggering effect on ^{154}Dy and ^{154}Dy.

help of the available experimental data [13,14].

$$S\,t\,(I) = 6\,\Delta E\,(I) - 4\,\Delta E\,(I-1) - 4\,\Delta E\,(I+1) + \\ + \Delta E\,(I+2) + \Delta E\,(I-2)\,, \tag{11}$$

with

$$\Delta E\,(I) = E\,(I+1) - E\,(I)\,. \tag{12}$$

The calculated staggering patterns are illustrated in Fig. 6 and show an interaction between the positive and negative parity states for the ground state band of ^{154,156}Dy.

3.4 Back bending

The moment of inertia J and energy parameters $\hbar\omega$ are calculated using (13) and (14):

$$\frac{2J}{\hbar^2} = \frac{4I-2}{\Delta E(I \to I-2)}\,, \tag{13}$$

$$(\hbar\omega)^2 = (I^2 - I + 1)\left[\frac{\Delta E(I \to I-2)}{(2I-1)}\right]^2\,. \tag{14}$$

The plots in Fig. 7 show forward bending for ^{154}Dy at $I^+ = 18$ and upper bending at $I^+ = 22$ for ^{156}Dy. Bending in higher states may be explained as due to band crossing.

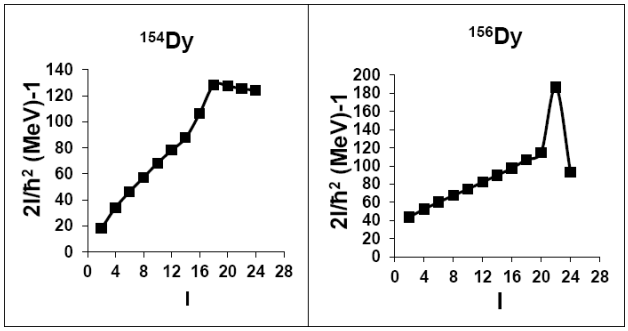

Fig. 7: Back bending ^{154}Dy and ^{156}Dy.

$I_i^+\ I_f^+\ I_{f}^{\prime +}$	^{154}Dy	^{156}Dy
$0_2\ 0_1\ 2_1$	0.0778	0.3526
$0_3\ 0_2\ 2_2$	0.2455	0.0285
$0_3\ 0_1\ 2_2$	0.0108	6.9000
$0_4\ 0_3\ 2_3$	0.1403	0.0000
$0_4\ 0_2\ 2_3$	0.0363	1.7686
$0_4\ 0_1\ 2_3$	0.0247	0.1903
$2_2\ 2_1\ 0_2$	2.4500	1.3870
$2_3\ 2_1\ 0_2$	0.2679	0.0454
$2_3\ 2_2\ 0_2$	0.1114	2.2727
$4_3\ 4_1\ 2_3$	0.0434	0.0785
$4_3\ 4_2\ 2_3$	0.0193	1.4117
$4_4\ 4_1\ 2_3$	0.0303	0.3177
$4_4\ 4_2\ 2_3$	5.3636	0.254
$4_2\ 4_1\ 2_2$	0.2384	0.0027
$6_2\ 6_1\ 4_2$	0.2422	0.1347
$8_2\ 8_1\ 6_2$	0.0609	0.0173
$10_2\ 10_1\ 8_2$	0.0337	0.0134

Table 5: $X_{if'f}\,(E0/E2)$ ratios in ^{154,156}Dy.

3.5 Electric monopole transitions

The electric monopole transitions, $E0$, are normally occurring between two states of the same spin and parity by transferring energy and zero unit of angular momentum. The strength of the electric monopole transition, $X_{if'f}\,(E0/E2)$ [17] can be calculated using (15) and (16) and are presented in Table 5

$$X_{if'f}\,(E0/E2) = \frac{B\,(E0, I_i - I_f)}{B\,(E2, I_i - I_{f})}\,, \tag{15}$$

where $I_i = I_f$=0, I_{f}=2 and $I_i = I_f \neq 0$, $I_f = I_{f}$.

$$X_{if'f}\,(E0/E2) = (2.54\times10^9)\,A^{3/4}\,\frac{E_\gamma^5(\mathrm{MeV})}{\Omega_{KL}}\times \\ \times\alpha(E2)\,\frac{T_e(E0, I_i - I_f)}{T_e(E_2, I_i - I_{f})}\,, \tag{16}$$

A : mass number;
I_i : spin of the initial state where $E0$ and $E2$ transitions are depopulating it;
I_f : spin of the final state of $E0$ transition;
$I_{'f}$: spin of the final state of $E2$ transition;
E_γ : gamma ray energy;
Ω_{KL} : electronic factor for K, L shells [18];
$\alpha(E2)$: conversion coefficient of the $E2$ transition;
$T_e(E0, I_i - I_f)$: absolute transition probability of the $E0$ transition between I_i and I_f states; and
$T_e(E_2, I_i - I_{'f})$: absolute transition probability of the $E2$ transition between I_i and $I_{'f}$ states.

Unfortunately, there is no experimental data available for comparison with the calculated values.

3.6 Conclusions

The *IBA*-1 model has been applied successfully to ^{154,156}Dy isotopes and:

1. Levels' energy are successfully reproduced;
2. Potential energy surfaces are calculated and show vibrational-like characteristics to ^{154}Dy and slight prolate deformation to ^{156}Dy;
3. Electromagnetic transition rates $B(E1)$ and $B(E2)$ are calculated;
4. Bending has been observed at $I^+ = 18$ for ^{154}Dy and at $I^+ = 22$ for ^{156}Dy ;
5. Staggering effect has been calculated and beat patterns observed which show an interaction between the positive and negative parity states;
6. Strength of electric monopole transitions $X_{if'f}(E0/E2)$ are calculated; and
7. The potential energy surfaces, transition probability rates and energy show that ^{156}Dy has the $X(5)$ symmetry.

Received on November 28, 2017

References

1. Chabab M., El Batoul A., Hamzavi M., Lahbas A., Oulne M. Excited collective states of nuclei within Bohr Hamiltonian with Tietz-Hua potential. *Eur. Phys. J. A*, 2017, v. 53, 157.
2. Buganu1 P. and Budaca R. Sextic potential for γ-rigid prolate nuclei. *J. Phys. G*, 2015, v. 42, 105106.
3. Alimohammadi M., Zare S. Investigation of Bohr-Mottelson Hamiltonian in γ-rigid version with position dependent mass. *Nucl. Phys. A*, 2017, v. 960, 78.
4. Xiao-Dong Sun, Ping Guo, and Xiao-Hua Li. Systematic study of α-decay half-lives for even-even nuclei within a two-potential approach. *Phys. Rev. C*, 2016, v. 93, 034316.
5. Li1 Z. P., Niksic T. and Vretenar D. Coexistence of nuclear shapes: self-consistent mean-field and beyond. *J. Phys. G*, 2015, v. 43, 024005.
6. Girija K. K. Role of shape and quadrupole deformation of parents in the cluster emission of rare earth nuclei. *Int. J. Mod. Phys. E*, 2014, v. 23, 1450002.
7. Zimba G. L., Sharpey-Schafer J. F., Jones P., Bvumbi S. P., Masiteng L. P., Majola S. N. T., Dinoko T. S., Lawrie E. A., Lawrie J. J., Negi D., Papka P., Roux D., Shirinda O., Easton J. E., Khumalo N. A. Octupole correlations in N=88 ^{154}Dy: Octupole vibration versus stable deformation. *Phys. Rev. C*, 2016, v. 94, 054303.
8. Ijaz Q. A., Ma W. C., Abusara H., Afanasjev A. V., Xu Y. B., Yadav R. B., Zhang Y. C., Carpenter M. P., Janssens R. V. F., Khoo T. L., Lauritsen T., Nisius D. T. Excited superdeformed bands in ^{154}Dy and cranked relativistic mean field interpretation. *Phys. Rev. C*, 2009, v. 80, 034322.
9. Paul E. S., Rigby S. V., Riley M. A., Simpson J., Appelbe D. E., Campbell D. B., Choy P. T. W., Clark R. M., Cromaz M., Evans A. O., Fallon P., Gorgen A., Joss D. T., Lee I. Y., Macchiavelli A. O., Nolan P. J., Pipidis A., Ward D., Ragnarsson I. Loss of collectivity in the transitional ^{156}Er nucleus at high spin. *Phys. Rev. C*, 2009, v. 79, 044324.
10. Blasi N., Atanasova L., Balabanski D., Das Gupta S., Gladinski K., Guerro L., Nardelli S., and Saltarelli A. $E0$ decay from the first 0^+ state in ^{156}Dy and ^{160}Er. *Phys. Rev. C*, 2014, v. 90, 044317.
11. Scholten O. The program package PHINT (1980) version. Internal report KVI-63, Keryfysisch Versneller Institut, Gronigen, 1979.
12. Ginocchio J. N. and Kirson M. W. An intrinsic state for the interacting boson model and its relationship to the Bohr- Mottelson approximation. *Nucl. Phys. A*, 1980, v. 350, 31.
13. Reich C. W. ADOPTED LEVELS, GAMMAS for ^{154}Dy. *Nuclear Data Sheets*, 2009, v. 110, 2257.
14. Reich C. W. ADOPTED LEVELS, GAMMAS for ^{156}Dy. *Nuclear Data Sheets*, 2012, v. 113, 2537.
15. Pritychenko B., Birch M., Singh B. and Horoi M. Tables of $E2$ transition probabilities from the first 2^+ states in even-even nuclei. *Atomic Data and Nuclear Data Tables*, 2016, v. 107, 1.
16. Minkov N., Yotov P., Drenska S. and Scheid W. Parity shift and beat staggering structure of octupole bands in a collective model for quadrupole-octupole deformed nuclei. *J. Phys. G*, 2006, v. 32, 497.
17. Rasmussen J. O. Theory of $E0$ transitions of spheroidal nuclei. *Nucl.Phys.*, 1960, v. 19, 85.
18. Bell A. D., Aveldo C. E., Davidson M. G. and Davidson J. P. Table of $E0$ conversion probability electronic factors. *Can. J. Phys.*, 1970, v. 48, 2542.